Air Stable *n*-Channel Organic Semiconductors for Thin Film Transistors Based on Fluorinated Derivatives of Perylene Diimides

H. Z. Chen,*[,†,‡] M. M. Ling,[‡] X. Mo,[†] M. M. Shi,[†] M. Wang,[†] and Z. Bao*[,‡]

Department of Polymer Science and Engineering, State Key Lab of Silicon Materials, Zhejiang University, Hangzhou 310027, People's Republic of China, and Department of Chemical Engineering, Stanford University, 381 North South Mall, Stanford, California 94305-5025

Received October 2, 2006. Revised Manuscript Received December 18, 2006

A series of *n*-type organic semiconductors based on perylene diimides were synthesized. These materials were fully characterized by FTIR and UV−vis spectra as well as elemental analysis. Thin film transistors (TFTs) using a top-contact geometry were fabricated by vapor deposition of these perylene diimide derivatives as the semiconductive channel on surface treated SiO_2/Si substrates at various substrate temperatures. The measured TFT performance depended heavily on the type and the number of substituents. We found higher field-effect mobilities for compounds with stronger electron-withdrawing substituents. TFTs with fluorinated perylene diimides showed much better performance in air than a chlorinated derivative. The highest mobility, ca. 0.068 cm^2/V s, was measured for the compound with the most fluorine substituents (i.e., *N*,*N*′-diperfluorophenyl-3,4,9,10-perylenetetracarboxylic diimide (**8**)). The effect of molecular structure on film morphology was observed using an atomic force microscope (AFM). The correlation between the number of fluorine substitutions and the TFT air stability was studied. Our results showed better device air stability for compounds with more fluorine substituents, due to their lower LUMO energy levels. Other factors affecting TFT performance, such as substrate temperature and SiO_2 dielectric surface treatment, were also investigated.

Introduction

Organic semiconductors have been intensively investigated during the past 20 years because of their potential applications in many areas, such as field-effect transistors (FETs),[1] light-emitting displays,[2] and photovoltaic cells.[3] All of these applications require both hole-transporting (*p*-type) and electron-transporting (*n*-type) materials with suitable physical, chemical, electrical, and/or photochemical properties. Although organic thin film transistors (OTFTs) have been investigated for many years, most studies so far have been focused on developing *p*-channel semiconductors, such as pentacene and oligothiophenes derivatives. A hole mobility greater than 1 cm^2/V s has been reported for pentacene.[4] For realization of organic complementary metal−oxide semiconductor (CMOS) circuits, both *p*- and *n*-channel semiconductors are required.[5] Therefore, it is important to have high-performance *n*-channel materials. The main problem for most currently known *n*-channel materials is their low charge carrier mobility, which is also one of the key factors limiting the development of high-performance organic solar cells and light-emitting diodes.[6]

* Corresponding authors. E-mail: (H.Z.C.) hzchen@zju.edu.cn and (Z.B.) zbao@stanford.edu.

† Zhejiang University.

‡ Stanford University.

(1) (a) Facchetti, A.; Yoon, M.-H.; Stern, C. L.; Hutchison, G. R.; Ratner, M. A.; Marks, T. J. *J. Am. Chem. Soc.* **2004**, *126*, 13480. (b) Merlo, J. A.; Newman, C. R.; Gerlach, C. P.; Kelley, T. W.; Muyres, D. V.; Fritz, S. E.; Toney, M. T.; Frisbie, C. D. *J. Am. Chem. Soc.* **2005**, *127*, 3997. (c) Ling, M. M.; Bao, Z. *Chem. Mater.* **2004**, *16*, 4824. (d) Bao, Z.; Lovinger, A. J.; Dodabalapour, A. *Adv. Mater.* **1997**, *9*, 42. (e) Meng, H.; Bao, Z.; Lovinger, A. J.; Wang, B.-C.; Mujsce, A. M. *J. Am. Chem. Soc.* **2001**, *123*, 9214. (f) Siegrist, T.; Fleming, R. M.; Haddon, R. C.; Laudise, R. A.; Lovinger, A. J.; Katz, H. E.; Bridenbaugh, P.; Davis, D. D. *J. Mater. Res.* **1995**, *10*, 2170. (g) Li, X. C.; Sirringhaus, H.; Garnier, F.; Holmes, A. B.; Moratti, S. C.; Feeder, N.; Clegg, W.; Teat, S. J.; Friend, R. H. *J. Am. Chem. Soc.* **1998**, *120*, 2206. (h) Podzorov, V.; Sysoev, S. E.; Loginova, E.; Pudalov, V. M.; Gershenson, M. E. *Appl. Phys. Lett.* **2003**, *83*, 3504. (i) Meng, H.; Sun, F.; Goldfinger, M. B.; Jaycox, G. D.; Li, Z.; Marshall, W. J.; Blackman, G. S. *J. Am. Chem. Soc.* **2005**, *127*, 2406.

(2) (a) Tang, C. W.; VanSlyke, S. A. *Appl. Phys. Lett.* **1987**, *51*, 913. (b) Burroughes, J. H.; Bradley, D. D. C.; Brown, A. R.; Marks, R. N.; Mackay, K.; Friend, R. H.; Burns, P. L.; Holmes, A. B. *Nature* **1990**, *347*, 539. (c) Braun, D.; Heeger, A. J. *Appl. Phys. Lett.* **1991**, *58*, 1982. (d) Friend, R. H.; Gymer, R. W.; Holmes, A. B.; Burroughes, J. H.; Marks, R. N.; Taliani, C.; Bradley, D. D. C.; Dos Santos, D. A.; Brédas, J. L.; Lögdlund, M.; Salaneck, W. R. *Nature* **1999**, *397*, 121. (e) Kulkarni, A. P.; Tonzola, C. J.; Babel, A.; Jenekhe, S. A. *Chem. Mater.* **2004**, *16*, 4556. (f) Kido, J.; Okamoto, Y. *Chem. Rev.* **2002**, *102*, 2357.

(3) (a) Tang, C. W. *Appl. Phys. Lett.* **1986**, *48*, 183. (b) Liu, J.; Kadnikova, E. N.; Liu, Y.; McGehee, M.; Fréchet, J. M. J. *J. Am. Chem. Soc.* **2004**, *126*, 9486. (c) Yang, F.; Shtein, M.; Forrest, S. R. *Nat. Mater.* **2005**, *4*, 37. (d) Peumans, P.; Uchida, S.; Forrest, S. R. *Nature* **2003**, *425*, 158. (e) Breeze, A. J.; Salomn, A.; Ginley, D. S.; Gregg, B. A.; Tillmann, H.; Hörhold, H. H. *Appl. Phys. Lett.* **2002**, *81*, 3085. (f) Schmidt-Mende, L.; Fechtenkötter, A.; Müllen, K.; Moons, E.; Friend, R. H.; MacKenzie, J. D. *Science* **2001**, *293*, 1119. (g) Tan, L.; Curtis, M. D.; Francis, A. H. *Chem. Mater.* **2003**, *15*, 2272. (h) Yu, G.; Gan, J.; Hummelen, J. C.; Wudl, F.; Heeger, A. J. *Science* **1995**, *270*, 1789. (i) Dennler, G.; Lungenschmied, C.; Neugebauer, H.; Sariciftci, N. S.; Labouret, A. *J. Mater. Res.* **2005**, *20*, 3224. (j) Li, G.; Shrotriya, V.; Huang, J. S.; Yao, Y.; Moriarty, T.; Emery, K.; Yang, Y. *Nat. Mater.* **2005**, *4*, 864.

(4) (a) Kelly, T. W.; Boardman, L. D.; Dunbar, T. D.; Muyres, D. V.; Pellerite, M. J.; Smith, T. P. *J. Phys. Chem. B* **2003**, *107*, 5877. (b) Klauk, H.; Halik, M.; Zschieschang, U.; Eder, F.; Schmid, G.; Dehm, C. *Appl. Phys. Lett.* **2003**, *82*, 4175. (c) Klauk, H.; Gundlach, D. J.; Nichols, J. A.; Sheraw, C. D.; Bonse, M.; Jackson, T. N. *Solid State Technol.* **2000**, *43*, 63.

(5) (a) Katz, H. E.; Johnson, J.; Lovinger, A. J.; Li, W. *J. Am. Chem. Soc.* **2000**, *122*, 7787. (b) Yoon, M.-H.; DiBenedetto, S. A.; Facchetti, A.; Marks, T. J. *J. Am. Chem. Soc.* **2005**, *127*, 1348.

10.1021/cm062352w CCC: $37.00
Published on Web 01/30/2007

Scheme 1. Synthesis of Perylene Diimides Derivatives 1−10

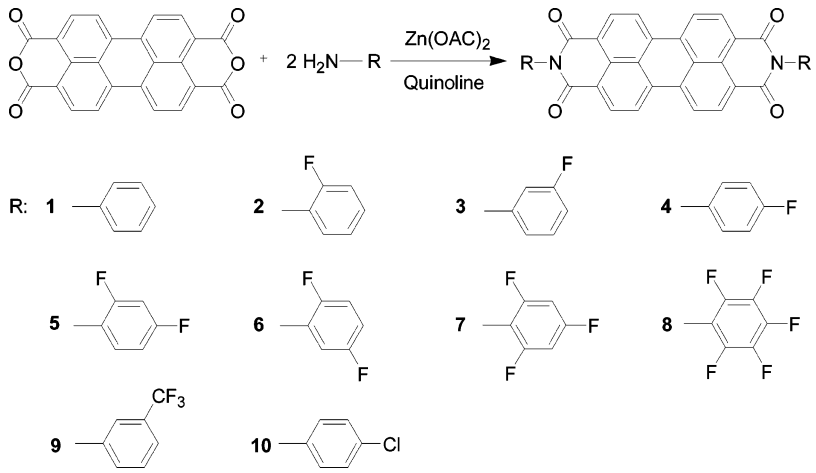

Several organic semiconductors with high electron mobility have been reported: (a) fullerene C_{60} and its derivatives,[7] (b) naphthalene and perylene diimide derivatives,[8] and (c) substituted oligothiophene derivatives.[9] A simple model of a Schottky-type injection barrier picture based on the relative HOMO and LUMO levels was used to explain *p*- or *n*-type majority carrier activity in perfluoroalkyl- and alkyl-functionalized oligothiophenes.[9a] However, OTFT devices fabricated with some of the previous *n*-type materials without high electron-withdrawing substituents are air sensitive. The major charge carriers (i.e., electrons) are easily trapped by oxygen, leading to device degradation upon exposure to air. Developing organic *n*-channel materials with both high mobility and good stability in air remains a great challenge.

The current strategy to obtain air stable *n*-type organic semiconductors is introducing strong electron-withdrawing substituents onto a π-conjugated core by lowering its LUMO energy level so that the electron charge carriers are less susceptible to oxidation. Examples of such substitutions are cyano, fluoro, and perfluoroalkyl, etc. Several air stable *n*-type organic semiconductors based on this strategy have been reported.[10] The first successful demonstration of such a molecular design strategy involves perfluorinated metal phthalocyanines giving an electron mobility of 0.03 cm^2/V s in air.[10a] Higher mobilities have subsequently been demonstrated with fluorinated derivatives of naphthalene diimides.[8a] More recently, cyano and fluoroalkyl substituted perylene diimides were reported with an electron mobility of 0.64 cm^2/V s in air. [8]

In this study, we prepared a series of *n*-type organic semiconductors based on perylene diimides as shown in Scheme 1. Electron-withdrawing groups, such as F, CF_3, and Cl, were introduced into the two phenyl substituents on perylene diimides. By changing the number and position of the substituents, we systematically investigated the effect of chemical structural variation on molecular energy level, electron mobility, and transistor stability.

Experimental Procedures

Syntheses and Material Characterization. The syntheses and chemical structures are depicted in Scheme 1. Compounds **1**[12] and **8**[10b] were reported previously and were prepared according to literature procedures. The other perylene diimide derivatives were prepared according to procedures described in refs 5a and 11. Details of the synthetic process and characterization are described in the Supporting Information.

Device Fabrication. Highly doped *n*-type Si (100) wafers (<0.004 Ω cm) were used as substrates. A SiO_2 layer (capacitance per unit area C_i = 10 nF/cm^2) as a gate dielectric was thermally grown to 3000 Å onto the Si substrates. Three different surface treatments for SiO_2/Si substrates were performed after they were rinsed with acetone followed by isopropyl alcohol: (a) *n*-octadecyl triethoxysilane [$C_{18}H_{37}Si(OC_2H_5)_3$, OTS, obtained from Aldrich Chem. Co.] treatment: a few drops of OTS was loaded on top of a preheated quartz plate (~90 °C) to generate OTS vapor in a

(6) (a) Shaheen, S. E.; Ginley, D. S.; Jabbour, G. E. *MRS Bull.* **2005**, *30*, 10. (b) Kulkarni, A. P.; Tonzola, C. J.; Babel, A.; Jenekhe, S. A. *Chem. Mater.* **2004**, *16*, 4556.

(7) (a) Frankevich, E.; Maruyama, Y.; Ogata, H. *Chem. Phys. Lett.* **1993**, *214*, 39. (b) Jarrett, C. P.; Pichler, K.; Newbould, R.; Friend, R. H. *Synth. Metal* **1996**, *77*, 35. (c) Shimada, T.; Koma, A. *Jpn. J. Appl. Phys., Part 1* **2002**, *41*, 2724. (d) Kobayashi, S.; Takenobu, T.; Mori, S.; Fujiwara, A.; Iwasa, Y. *Appl. Phys. Lett.* **2003**, *82*, 4581. (e) Meijer, E. J.; De Leeuw, D. M.; Setayesh, S.; van Veenendaal, E.; Huisman, B. H.; Blom, P. W. M.; Hummelen, J. C.; Scherf, U.; Klapwijk, T. M. *Nat. Mater.* **2003**, *2*, 678. (f) Haddon, R. C.; Perel, A. S.; Morris, R. C.; Palstra, T. T. M.; Hebard, A. F.; Fleming, R. M. *Appl. Phys. Lett.* **1995**, *67*, 121. (g) Lee, T. W.; Byun, Y.; Koo, B. W.; Kang, I. N.; Lyu, Y. Y.; Lee, C. H.; Pu, L.; Lee, S. Y. *Adv. Mater.* **2005**, *17*, 2180.

(8) (a) Katz, H. E.; Lovinger, A. J.; Johnson, J.; Kloc, C.; Siegrist, T.; Li, W.; Lin, Y. Y.; Dodabalapur, A. *Nature* **2000**, *404*, 478. (b) Malenfant, P. R. L.; Dimitrakopoulos, C. D.; Gelorme, J. D.; Kosbar, L. L.; Graham, T. O.; Curioni, A.; Andreoni, W. *Appl. Phys. Lett.* **2002**, *80*, 2517. (c) Ranke, P.; Bleyl, I.; Simmerer, J.; Haarer, D.; Bacher, A.; Schmidt, H. W. *Appl. Phys. Lett.* **1997**, *71*, 1332. (d) Law, K. Y. *Chem. Rev.* **1993**, *33*, 449. (e) Chesterfield, R. J.; McKeen, J.; Newman, C. R.; Frisbie, C. D. *J. Appl. Phys.* **2004**, *95*, 6396. (f) Laquindanum, J. G.; Katz, H. E.; Dodabalapur, A.; Lovinger, A. J. *J. Am. Chem. Soc.* **1996**, *118*, 11331. (g) Jones, B. A.; Ahrens, M. J.; Yoon, M.; Facchetti, A.; Marks, T. J.; Wasielewski, M. R. *Angew. Chem., Int. Ed.* **2004**, *43*, 6363.

(9) (a) Facchetti, A.; Mushrush, M.; Yoon, M.-H.; Hutchison, G. R.; Ratner, M. A.; Marks, T. J. *J. Am. Chem. Soc.* **2004**, *126*, 13859. (b) Facchetti, A.; Mushrush, M.; Katz, H. E.; Marks, T. J. *Adv. Mater.* **2003**, *15*, 33. (c) Facchetti, A.; Deng, Y.; Wang, A. C.; Koide, Y.; Sirringhaus, H.; Marks, T. J.; Friend, R. H. *Angew. Chem., Int. Ed.* **2000**, *39*, 4547.

(10) (a) Bao, Z.; Lovinger, A. J.; Brown, J. *J. Am. Chem. Soc.* **1998**, *120*, 207. (b) Shi, M. M.; Chen, H. Z.; Sun, J. Z.; Ye, J.; Wang, M. *Chem. Commun.* **2003**, *14*, 1710.

(11) Katz, H. E.; Lovinger, A. J.; Johnson, J.; Kloc, C.; Siegrist, T.; Li, W.; Lin, Y. Y.; Dodabalapur, A. *Nature* **2000**, *404*, 478.

(12) Horowitz, G.; Kouki, F.; Spearman, P.; Fichou, D.; Nogues, C.; Pan, X.; Garnier, F. *Adv. Mater.* **1996**, *8*, 242.

vacuum desiccator with cleared SiO_2/Si substrates inside. The desiccator was immediately pumped under a house vacuum, and the SiO_2/Si substrates were exposed to OTS vapor under vacuum for 5 h. Finally, the substrates were baked at 110 °C for 15 min, rinsed with toluene, and dried with a stream of air; (b) hexamethyldisilazane [$(CH_3)_3$-Si-N-Si-$(CH_3)_3$), HMDS] treatment: an yield enhancement system (YES-100) was used; and (c) poly(α-methylstyrene) (PMSt, typical $M_n = 4000$, $T_g = 76$ °C, from Aldrich Chem. Co.) treatment: an ultrathin PMSt layer of 10 nm thickness was spin-coated from its 0.1 wt % solution in toluene, according to literature procedures.[13]

The organic semiconductor thin films (40 nm) were vacuum deposited on SiO_2/Si substrates held at either room temperature (rt) or elevated temperatures (i.e., 75, 125, 165, and 200 °C) with a deposition rate of 0.5 Å/s and under a vacuum of 10^{-6} Torr. The film thickness was monitored by a quartz crystal microbalance. The morphology of the thin films was observed in tapping mode by a DI 3000 atomic force microscope (AFM) from Digital Instruments Inc.

Top-contact devices (see Figure 3, inset) were fabricated by evaporating gold source and drain electrodes onto the organic semiconductor films through a shadow mask.

Device Characterization. The electrical characteristics of OTFT devices were measured using a Keithley 4200-SCS semiconductor parameter analyzer. The measurements were carried out both inside a nitrogen glove box (H_2O less than 0.1 ppm and O_2 less than 1 ppm) immediately after they were prepared without any exposure to air and under an ambient atmosphere condition (the typical relative humidity level is between 30 and 50%) after the devices were exposed to air for a certain amount of time. The calculation for key device parameters, including charge carrier mobility (μ), on/off current ratio (I_{on}/I_{off}), and threshold voltage (V_t), is described in the Supporting Information. All data listed in the paper are average values from at least three devices on each of the 10 samples.

Results and Discussion

Syntheses and Characterization of Perylene Diimide Derivatives. A series of perylene diimide derivatives were readily synthesized using a one-step reaction from substituted aniline derivatives and commercially available PTCDA. The synthetic route and chemical structures of compounds prepared for this study are shown in Scheme 1. Three kinds of substituents (i.e., F, CF_3, and Cl) were used as the aniline derivatives. By changing the number and/or the position of the substituents, 10 compounds abbreviated as compounds **1**−**10** were obtained. The purity of the compounds was determined by elemental analysis, which is in good agreement with the calculated values, indicating that these perylene diimide derivatives are obtained in good purity.

The −C═O stretching band for the carbonyl group of substituted perylene diimides **2**−**10** was shifted to a longer wavenumber as compared to that of **1**. A slight shift was observed in compounds of **2**, **3**, **4**, **9**, and **10** with a mono-substituent, while the biggest shift was seen for compound **8** with pentafluoro substitution on the phenyl ring. The shift increases with an increasing number of fluoro substituents. This can be interpreted in terms of the inductive effect of F atoms. By increasing the number of the highly electronegative F substituent on phenyl groups, the electron-withdrawing capability of the F substituted phenyl groups was enhanced; thus, the sharing of the lone pair electrons on the N atom of the vicinal imide group with the carbon atom of the carbonyl group was weakened, and subsequently, the double bond of the carbonyl group was enhanced, leading to a higher vibrational frequency for the −C═O stretching band.

Table 1. Summary of Optical Absorption Wavelengths, Redox Potentials (Measured by Cyclic Voltammetry), and LUMO Energy Levels for Perylene Diimide Derivatives

compound	λ_{abs} (nm)[a]	$E_{ox,1}$ (eV)[b]	$E_{red,1}$ (eV)[b]	$E_{red,1}{}^{-1}{}_{1/2}$ (eV)[b]	LUMO (eV)[c]
1	524, 488, 457	−0.64	−0.52	−0.58	−4.16
2	524, 488, 458	−0.63	−0.49	−0.56	−4.18
3	523, 489, 458	−0.57	−0.53	−0.55	−4.19
4	524, 488, 458	−0.57	−0.54	−0.56	−4.18
5	526, 490, 459	−0.58	−0.45	−0.52	−4.22
6	525, 489, 459	−0.55	−0.45	−0.50	−4.24
7	528, 491, 460	−0.58	−0.45	−0.51	−4.23
8	529, 493, 461	−0.51	−0.43	−0.47	−4.27
9	524, 489, 458	−0.63	−0.48	−0.55	−4.19
10	524, 489, 458	−0.66	−0.50	−0.58	−4.16

[a] Measured in DMF solution. [b] Versus SCE and determined from differential curves. [c] Determined using $E_{red,1}{}^{-1}{}_{1/2}$ according to literature methods.[16]

Table 1 summarizes the optical absorption peaks obtained in DMF solutions and the LUMO energy levels calculated from cyclic voltammetry (CV) for **1**−**10**. Compound **1** shows three major absorption peaks at 524, 488, and 457 nm in solution, respectively. These peaks are assigned to the $\pi-\pi^*$ transitions for the perylene core.[14] The five monosubstituted perylene diimide derivatives **2**, **3**, **4**, **9**, and **10** show rather similar absorption spectra as that of **1** regardless of whether the substituent is F, CF_3, or Cl. But, the absorption is slightly red-shifted with an increasing number of F groups, which can be explained by the increased solvation due to the increased molecular polarity of the compounds substituted by more high electronegative F groups.[10b,15]

The energy levels of perylene diimide derivatives were estimated based on CV results. Their LUMO energy levels were calculated based on the electrochemical reduction potentials. The relative LUMO level depends on the type of substituent and its position. The introduction of a Cl substituent at the 4-position of the phenyl group (**10**) does not change the LUMO level as compared to its unsubstituted counterpart **1**, while the LUMO level is lowered by 0.02 eV if the more electronegative F group is substituted at the same position (**4**). CF_3 substitution (**9**) results in about the same LUMO level as F substitution (**3**) at the same 3-position. Compound **3** with a mono-F substituent at the 3-position has a slightly lower LUMO level (−4.19 eV) than that at the 2- or 4-positions (−4.18 eV). Cyclic voltammograms of **1**, **2**, **5**, **7**, and **8** with no, mono-, di-, tri-, and penta-F substituents are illustrated in Figure 1. The lower curve of the CV is the forward scan, and the reverse scan is the one above it. It can be seen that their half-wave potential ($E^{-1}{}_{1/2}$) versus SCE for the first reduction peak is shifted toward more positive values and becomes more reversible with an increasing number of substituted F atoms, and consequently, the LUMO

(13) Kelley, T. W.; Muyres, D. V.; Baude, P. F.; Smith, T. P.; Jones, T. D. *Mater. Res. Soc. Symp. Proc.* **2003**, *771*, L6.5.1.

(14) (a) Cormier, R. A.; Greeg, B. A. *J. Phys. Chem. B* **1998**, *10*, 1309. (b) Graser, F.; Hädicke, E. *Liebigs Ann. Chem.* **1980**, 1994.

(15) Shi, M. M.; Chen, H. Z.; Shi, Y.; Sun, J. Z.; Wang, M. *J. Phys. Chem. B* **2004**, *108*, 5901.

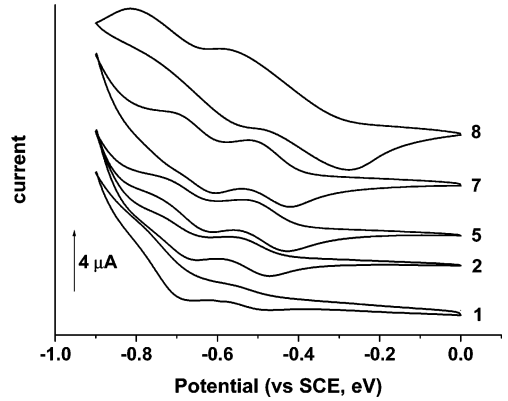

Figure 1. Cyclic voltammograms of **1**, **2**, **5**, **7**, and **8** with no-, mono-, di-, tri-, and penta-F substituents measured in CH_2Cl_2 solution with a scanning rate of 50 mV/s. The lower curve of the CV is the forward scan, and the reverse scan is the one above it.

energy level decreases with the number of F atoms. The LUMO levels of compounds **1**, **2**, **5**, **7**, and **8** with no, mono-, di-, tri-, and penta-F substituents determined from the electrochemical data are −4.16, −4.18, −4.22, −4.23, and −4.27 eV, respectively.[16] The lowering of the LUMO levels of the corresponding materials by multiple fluorination suggests that the anion forms of these compounds are more stable toward oxidation with an increased number of F atoms.

Influence of Fluorination on TFT Performance. To investigate how fluorination affects OTFT performance, OTFTs with compounds **1**−**10** deposited on OTS−SiO_2 at a 125 °C substrate temperature were prepared, and their TFT performance results, including field-effect mobility (μ_e), on/off current ratio (I_{on}/I_{off}), and threshold voltage (V_t) obtained from current−voltage characteristics of the drain current as a function of gate voltage, are summarized in Table 2. The device measurements were carried out both inside a glove box and under an ambient atmosphere after exposure to air for 1 h. As expected, all of the compounds showed typical *n*-channel transistor characteristics as an increasing source-drain current under an increasing positive gate bias was observed. For all compounds except compound **1**, the mobility and on/off ratio did not change when the device was measured immediately after being taken out of the N_2 glove box.

We first investigated how the type of substitution species, such as F, CF_3, and Cl used in this study, affects TFT performance. From Table 2, we note that **3** with mono-F has a 1 order of magnitude higher mobility than that of **9** with mono-CF_3 at the same position when tested both in the N_2 glove box and in the ambient atmosphere. However, the other two compounds **2** and **4** with a mono-F group at a different position exhibited a higher mobility when tested in the N_2 glove box but still at the same order of magnitude as that of **9** in ambient atmosphere. It can also be seen that **4** with mono-F has a higher electron mobility than that of **10** with mono-Cl at the same position when tested both inside and outside the glove box. These observations indicate that fluorination can lead to better OTFT performance in both inert and ambient atmosphere than chlorination due to the lower LUMO level caused by the higher electronegativity of the F atom. The percentage drop of average mobility after moving the device out from the glove box to air is 26, 45−85, and 96% for the CF_3, F, and Cl substituents, respectively. The CF_3 substituent resulted in the lowest LUMO level among the mono-substituted compounds reported here and the least percentage drop in the TFT mobility, indicating that CF_3 may be the most favorable substituent for air stable TFT performance among these three kinds of substituents.

Next, we compare the TFT performance of compounds **2**−**4**, which are substituted by one F group but at different positions. We found that **3** had the best TFT performance when tested both in the N_2 glove box and in air. However, there was no significant difference in the percentage drop of average mobility after moving devices out from glove box to air (43−85%). For compounds **5** and **6** with di-F substituents at the 2,4- and 2,5-positions on the N substituted phenyl rings, respectively, an increase in mobility by almost 1 order of magnitude, reaching 10^{-2} cm^2/V s, was observed when compared with those of monosubstituted derivatives. Both **5** and **6** showed not only higher mobility but also high on/off ratios in the order of 10^5 and 10^6. Another important observation for **5** and **6** was that there was a negligible change in mobility and on/off ratio after the devices were exposed to air for 1 h, indicating dramatic improvement in air stability due to the existence of the higher number of electron-withdrawing F atoms. When the N substituted phenyl was completely fluorinated (**8**), electron mobility as high as 0.058 cm^2/V s (in the glove box) and 0.043 cm^2/V s (in air) was obtained with on/off ratios in the range of 10^5. These results demonstrate that both OTFT performance and air stability are improved by increasing the number of substituted fluorine groups.

The threshold voltage (V_t) is compared among the fluorinated derivatives of perylene diimides. From Table **2**, it can be seen that V_t decreases significantly while increasing the number of substituted fluorine groups. A much lower V_t of 0.8 V (in the glove box) and 2 V (in air) was observed for **8** when compared to that of unsubstituted compound **1** (17 V in the glove box and 30 V in air). This suggests that the generation of the electron charge carriers in **8** is much easier, which is related to the lower gate voltage needed to fill in trap states due to the lowest LUMO level of **8**. The change of V_t between the devices tested in the glove box versus air might be caused by absorption of oxygen traps in air, which requires a higher gate voltage to fill in the additional traps, leading to a higher V_t for the devices tested in air. Compound **8** showed the smallest change in V_t after being taken from the glove box into air because it has the lowest LUMO level and because the electrons in LUMO are the least likely trapped.

The out-of-plane X-ray diffraction (XRD) measurements of various 40 nm fluorinated derivative thin films deposited on the 125 °C substrate with OTS surface treatment have been carried out. Table 3 summarizes the XRD peaks and *d* spacing for the thin films of compounds **1**−**10** (the XRD patterns for all compounds can be found in Figure S1 in the Supporting Information). The unsubstituted **1** shows a sharp primary peak at 5.15° with a *d* spacing of 17.14 Å for the

(16) Pommerehne, J.; Vestweber, H.; Guss, W.; Mahrt, R. F.; Bassler, H.; Porsch, M.; Daub, J. *Adv. Mater.* **1995**, *7* (6), 551.

Table 2. OTFT Performance Data for Devices with the Perylene Diimide Derivatives Grown on OTS Treated SiO_2 at 125 °C Substrate Temperature[a]

	in glove box			in ambient atmosphere			
compound	μ_e (cm^2/V s)[b]	I_{on}/I_{off}[c]	V_t (V)	μ_e (cm^2/V s)[b]	I_{on}/I_{off}[c]	V_t (V)	$\Delta\mu_e$ (%)[d]
1	0.017 ± 0.001	10^4	17−24	0.0025 ± 0.0007	10^3	30−52	85
2	$(1.9 \pm 0.01) \times 10^{-3}$	10^4	14−38	$(3.7 \pm 1.8) \times 10^{-4}$	10^4	41−57	81
3	$(3.8 \pm 2.2) \times 10^{-3}$	10^4	4−37	$(2.1 \pm 0.3) \times 10^{-3}$	10^4	41−51	45
4	$(2.1 \pm 0.3) \times 10^{-3}$	10^4	3−36	$(3.2 \pm 1.1) \times 10^{-4}$	10^3	21−49	85
5	0.012 ± 0.001	10^5	12−13	0.011 ± 0.001	10^5	14−19	8
6	0.031 ± 0.001	10^6	11−14	0.026 ± 0.002	10^6	23−24	16
7	0.03 ± 0.004	10^3	10−15	$(1.2 \pm 0.8) \times 10^{-3}$	10^3	11−50	96
8	0.056 ± 0.002	10^5	0.8−4	0.042 ± 0.001	10^5	2−6	25
9	$(3.1 \pm 0.2) \times 10^{-4}$	10^4	22−35	$(2.3 \pm 0.6) \times 10^{-4}$	10^4	27−46	26
10	$(7.0 \pm 1.0) \times 10^{-4}$	10^2	16−21	$(3.0 \pm 0.1) \times 10^{-5}$	10^2	45−48	96

[a] Measurements were carried out both inside he glove box and under ambient atmosphere (1 h after being exposed to an ambient environment). [b] Sweep range of V_g is from −60 to +100 V for $V_d = +100$ V. [c] On/off current ratio: calculated using I_d at $V_g = +100$ V and $V_d = +100$V divided by the lowest I_d (usually at $V_g \leq 0$ V). [d] Percentage drop of the average mobility, μ_e, after moving devices out of the glove box into air.

Table 3. Summary of the XRD Peaks and *d* Spacings for Films of Compounds 1−10

Compound	XRD peak 2θ (deg)	*d* spacing (Å)
1	5.15 (s)[a]	17.14
	10.35 (w)[b]	8.54
2	5.20 (s)	16.98
	8.35 (w)	10.58
	10.45 (w)	8.46
3	5.35 (s)	16.50
	6.25 (s)	14.13
	8.40 (w)	10.51
	11.75 (w)	7.52
	12.50 (w)	7.09
4	5.20 (s)	16.98
	10.50 (w)	8.42
5	4.95 (s)	17.83
	8.45 (w)	10.45
	10.05 (w)	8.79
6	4.90 (s)	18.01
	10.10 (w)	8.74
7	4.80 (s)	18.39
	9.65 (w)	9.15
8	5.05 (s)	17.48
	7.70 (w)	11.47
	10.15 (w)	8.71
9	4.95 (w)	17.84
	8.40 (w)	10.52
10	6.60 (w)	13.38
	8.50 (w)	10.39

[a] s: sharp peak. [b] w: weak peak (less than 400 counts/s).

(001) peak and a second weak peak with a *d* spacing of 8.54 Å for the (002) peak, which indicates that the molecules adapt an edge-on conformation in the thin film. For those compounds with mono-substitution, more peaks appear in addition to the <00*k*> peaks. For example, **3** shows more XRD peaks with *d* spacings of 16.50, 14.13, 10.51, 7.52, and 7.08 Å, respectively, which can be divided into two groups of 16.50, 10.51, and 7.52 Å and 14.13 and 7.09 Å. It is found that in the first group, the ratios of all *d* spacing to 16.50 Å are 1, 2/3, and 1/2, and in the second group, the ratios to 14.13 Å are 1 and 1/2. Compounds **9** and **10** have two weak peaks corresponding to the two phases. The weak XRD indicates the poor crystallinity for the films of compounds **9** and **10**. All these observations are consistent with the lower mobility of compounds **9** and **10**. As the number of substituted fluorine groups increases, compounds **5**−**8** show regular <00*k*> peaks with one sharp primary peak, which suggests the same molecular packing of edge-on conformation in these films as that of compound **1**, leading to high mobilities for these compounds.

A general trend is that, the higher the substrate temperature during thin film deposition, the higher the intensity of the XRD peak. There are fewer XRD peaks in the case of the room temperature substrate than the case with elevated substrate temperature. The high intensity of the diffraction peak indicates that the film has a good crystallinity. It correlates well with the charge carrier mobility results described in the following section.

We have also examined the morphology of thin films (40 nm thick) from different compounds using atomic force microscopy (AFM, images in Supporting Information Figure S2). However, no clear correlation between mobility of different compounds and their corresponding AFM topography images can be concluded, even though a clear trend for a given compound deposited at different substrate temperatures could be seen as discussed later in Figure 3. An in-depth study on the submonolayer morphology and thickness dependence of morphology is needed to look at the thin film morphology of the first 5 nm of films where the majority of charge carriers transport through. However, this is outside the scope of this paper and will be the subject of subsequent studies.

Influence of the Substrate Temperature on TFT Performance. It is known that the substrate temperature (T_s) used during organic semiconductor deposition plays an important role in the OTFT performance by affecting the nucleation and growth of the organic semiconductors.[1d,8g,9a,c] OTFTs from perylene diimide derivatives deposited at different T_s during thin film deposition were prepared to find the optimal substrate temperature. Table 4 summarizes the OTFT performance of **5** and **8** grown on an OTS treated SiO_2 surface at different T_s. For compound **8**, the mobility and on/off ratio initially increased with substrate temperature and slightly decreased above the optimal deposition temperature. The highest mobility (ca. 0.068 cm^2/V s) measured inside a N_2 glove box and 0.053 cm^2/V s measured in air were obtained when the T_s was 75 °C. V_t as low as 0.4 V in the glove box and 3 V in air was observed. The typical OTFT I_d versus V_{ds} characteristics of **8** deposited on OTS−SiO_2 at a 75 °C substrate temperature are shown in Figure 2. The TFT performance decreased slightly at higher T_s. The same trend is observed for TFTs fabricated with compound **5**, for which the best performance was obtained with a T_s of 125 °C. Its highest mobility and on/off ratio was around 0.012 cm^2/V s

Table 4. OFET Performance Data of 5 and 8 Grown on OTS Treated SiO_2 at Different Substrate Temperatures (T_s)[a]

		in glove box			in ambient atmosphere		
	T_s (°C)	μ_e (cm^2/V s)[b]	I_{on}/I_{off}[c]	V_t (V)	μ_e (cm^2/V s)[b]	I_{on}/I_{off}[c]	V_t (V)
5-OTS-SiO_2	Rt	$(6.0 \pm 0.1) \times 10^{-5}$	10^2	17−22	$(1.5 \pm 0.5) \times 10^{-5}$	10^2	12−39
	75	$(2.5 \pm 0.5) \times 10^{-3}$	10^3	4−28	$(1.5 \pm 0.5) \times 10^{-3}$	10^3	28−29
	125	0.012 ± 0.001	10^5	12−13	0.011 ± 0.001	10^5	14−19
	200	$(9.2 \pm 1.8) \times 10^{-3}$	10^4	8−13	$(4.4 \pm 1.7) \times 10^{-3}$	10^4	12−13
8-OTS-SiO_2	Rt	$(1.8 \pm 0.7) \times 10^{-4}$	<10	2	$(1.5 \pm 0.5) \times 10^{-4}$	<10	4−16
	75	0.066 ± 0.002	10^5	0.4−4	0.052 ± 0.001	10^5	3−6
	125	0.056 ± 0.002	10^5	0.8−4	0.042 ± 0.001	10^5	2−6
	200	0.060 ± 0.002	10^4	0.5−5	0.036 ± 0.001	10^4	3−7

[a] Measurements were carried out both inside a glove box and under ambient atmosphere (1 h after being exposed to an ambient environment). [b] Sweep range of V_g is from −60 to +100V for $V_d = +100$ V. [c] On/off current ratio: calculated using I_d at $V_g = +100$ V and $V_d = +100$ V divided by the lowest I_d usually at $V_g \leq 0$ V.

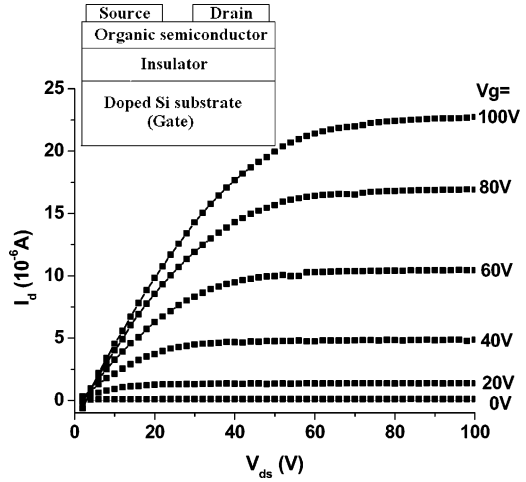

Figure 2. Typical I_d vs V_{ds} characteristics of compound **8** OTFT (on OTS treated SiO_2 at 75 °C substrate temperature). The measurements were carried out in ambient atmosphere (1 h after the device was exposed to an ambient environment). Inset: top-contact TFT geometry used in this work.

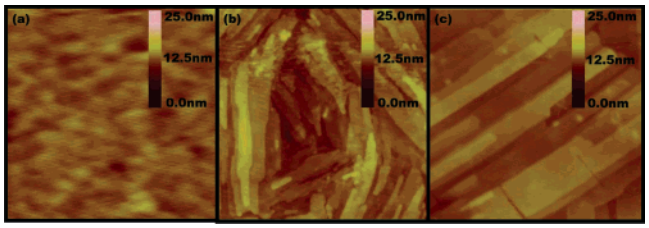

Figure 3. AFM topography images of 40 nm thin films of **5** deposited on OTS treated SiO_2 at various substrate temperatures: (a) room temperature (0.4 μm × 0.4 μm); (b) 125 °C (1.5 μm × 1.5 μm); and (c) 200 °C (1.5 μm × 1.5 μm).

and 10^5, respectively, both in the glove box and in air. If T_s is further increased to 200 °C, the TFT performance also decreases slightly. All other compounds in this study show similar trends as well.

It is noted that the best OTFT performance of compound **8** with penta-F can be reached at a relatively low substrate temperature of 75 °C as compared to that (125 °C) of other compounds in this paper. This feature is desirable for low cost device fabrication.

It is known that a higher substrate temperature during deposition generally leads to higher film crystallinity and larger grain sizes, both of which are desirable morphological features for increased mobility.[1c,d] As can be seen in Figure 3, which shows the tapping-mode AFM topographical images of compound **5** films deposited on OTS−SiO_2 at various substrate temperatures, the morphology of the film grown at room temperature consists of very small grains with an average size of 40 nm, and low mobility (ca. 6×10^{-5} cm^2/V s) was observed. When T_s increased to 125 °C, relatively large and densely packed rectangle grains with the size of about 200 nm × 1000 nm were formed, giving a high mobility (ca. 0.012 cm^2/V s). The slight decrease in mobility at a higher substrate temperature observed in this study may be related to cracks induced due to the mismatching in the thermal expansion coefficient between the substrate and the semiconductor. They are partially visible in some of the AFM images. For example, some cracks are observed in compound **5** thin films deposited at a high temperature of 200 °C shown in Figure 3c. Although well-ordered cuboid-shape grains are densely aligned on the substrate surface, the cracks present at such a high temperature reduce the mobility. Also, similar effects have been observed with other oligothiophene derivatives.[17] Charge transport in these fluorinated perylene dimide derivatives is dominated by the hopping mechanism, where the mobility is limited by trapping at grain boundaries.[18] The morphology of the thin films of **1**−**10** is shown in Figure S2 in the Supporting Information.

Influence of SiO_2 Surface Treatment on Mobility. The growth behavior of organic semiconductors depends not only on their chemical structure and the substrate temperature but also on the surface properties of the substrate on top of which they grow. In the top-contact TFT geometry used in this work, organic semiconductors were deposited on an inorganic insulator layer (i.e., SiO_2) on top of a Si substrate. Surface modification of SiO_2 with organo silane molecules has an impact on thin film morphology of organic semiconductors[19] as well as the threshold voltages.[20] By patterning dielectric surfaces with different surface modification molecules, selective deposition of organic semiconductors in desirable regions can be achieved,[21] which is important for the fabrication of integrated circuits. Moreover, recent studies have shown that Si−OH groups are traps for electrons

(17) Locklin, J.; Li, D. W.; Mannsfeld, S. C. B.; Borkent, E. J.; Meng, H.; Advincula, R.; Bao, Z. *Chem. Mater.* **2005**, *17*, 3366.
(18) Horowitz, G.; Hajlaoui, M. E. *Synth. Metal* **2001**, *122*, 185.
(19) Klauk, H.; Gundlach, D. J.; Nichols, J. A.; Sheraw, C. D.; Bonse, M.; Jackson, T. N. *Solid State Technol.* **2000**, *43*, 63.
(20) Kobayashi, S.; Nishikawa, T.; Takenobu, T.; Mori, S.; Shimoda, T.; Mitani, T.; Shimotani, H.; Yoshimoto, N.; Ogawa, S.; Iwasa, Y. *Nat. Mater.* **2004**, *3*, 317.
(21) (a) Briseno, A. L.; Aizenberg, J.; Han, Y.-J.; Penkala, R. A.; Moon, H.; Lovinger, A. J.; Kloc C.; Bao, Z. *J. Am. Chem. Soc.* **2005**, *127*, 12164. (b) Choi, H. Y.; Kim, S. H.; Jang, J. *Adv. Mater.* **2004**, *16*, 732. (c) Steudel, S.; Janssen, D.; Verlaak, S.; Genoe, J.; Heremans, P. *Appl. Phys. Lett.* **2004**, *85*, 5550.

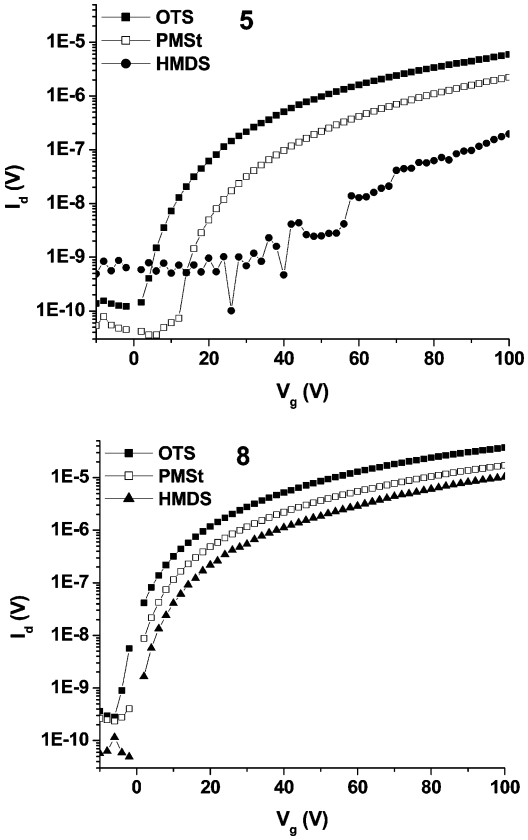

Figure 4. Transfer traces ($I_d - V_g$) of OTFTs based on **5** and **8** grown at $T_s = 125$ °C for $V_d = 100$V for devices with different surface treatments. The data were collected under ambient conditions after exposure to air for 1 h.

but not for holes.[22] Therefore, surface treatment of the SiO_2 layer is important to enhance OTFT performance by both improving the film growth of the organic semiconductors and reducing the electron trapping by Si−OH for *n*-type materials.[22]

Figure 4 presents transfer traces (I_d vs V_g) of OTFTs based on **5** and **8** deposited at $T_s = 125$ °C for $V_d = 100$ V. The SiO_2/Si substrates were treated with three types of materials, OTS, PMSt, and HMDS, before deposition of organic semiconductors. The OTFT measurements were carried out under ambient conditions after the devices were exposed to air for 1 h. We find that OTFTs with OTS surface treatment had the best performance in general, while OTFTs without any surface treatment gave the worst result. Our observation is in agreement with the report that Si−OH groups act as traps and that the traps are better passivated by OTS than HMDS.[22(b)]

Influence of Fluorination on Air Stability of OTFTs. We have demonstrated that high mobility can be obtained with our fluorinated perylene diimdes **5**, **6**, and **8** even after the devices had been exposed to air for 1 h. We also monitored their performance periodically after they were kept in ambient lab atmosphere, exposed to air and ambient light for an extended time. The electron mobilities of different compounds are plotted against time as shown in Figure 5.

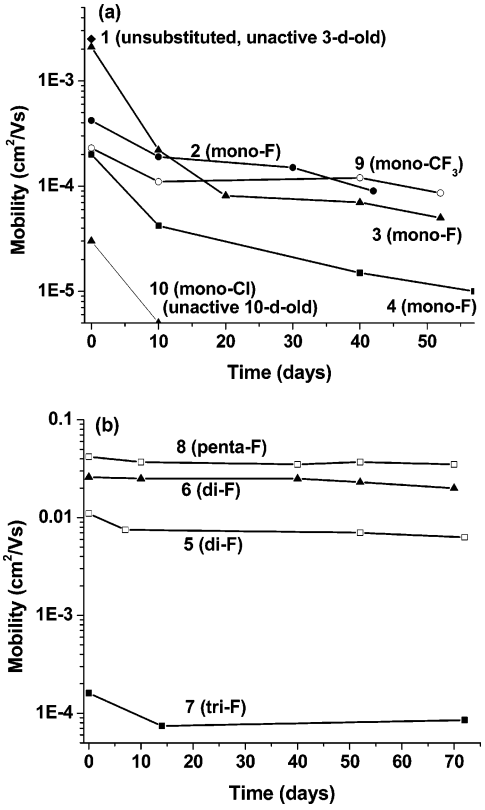

Figure 5. OTFT electron mobilities of **1**−**10** for $V_d = 100$ V as a function of time for devices exposed to air. The organic semiconductor films were grown on OTS treated SiO_2/Si substrates at $T_s = 125$ °C.

We first compare the air stability of OTFTs from different types of substituents: F, CF_3, and Cl. As mentioned earlier, the percentage drop of the average mobility, after moving devices that were made with compound **9** with a mono-CF_3 substituent grown on the OTS−SiO_2 substrate at 125 °C from the glove box to air, was the smallest among all mono-substituted derivatives. As can be seen from Figure 5a, its mobility also had the least percentage drop after the device had been exposed to air for 10 days. The mobility, on/off ratio, and threshold voltage of **9** showed negligible changes even after 40 days in air. The average mobility of **3** with mono-F when stored in air for the same amount of time, however, decreased by 1 order of magnitude after being exposed to air for 10 days. A similar trend was also observed for compounds **2** and **4** with mono-F at the 2- and 4-positions, respectively. Their mobility dropped 1 order of magnitude after being exposed to air for 40 days. For compound **10** (mono-Cl), the mobility was undetectable after 10 days. All these observations are consistent with the fact that the CF_3 group lowers the LUMO level of the resulting PTCDI compound **9** more than the other compounds.

Figure 5b shows the time dependence of electron mobility for compounds **5**−**8** with di-, tri-, and penta-F substitutions, respectively, deposited on OTS−SiO_2 substrates at $T_s = 125$ °C. The mobility of compound **5** initially decreased slightly faster and later did not change much over time in air for at least 72 days (further monitoring is in progress). The same trend was observed for compounds **6** and **7**. Remarkably, the mobility of compound **8** stayed almost constant over time in air for at least 72 days (further monitoring is in progress). The observed trend in device

(22) (a) Dimitrakopoulos, C. D.; Malenfant, P. R. L. *Adv. Mater.* **2002**, *14*, 99. (b) Chua, L.-L.; Zaumseil, J.; Chang, J.-F.; Ou, E. C.-W.; Ho, P. K.-H.; Sirringhaus, H.; Friend, R. H. *Nature* **2005**, *434*, 194.

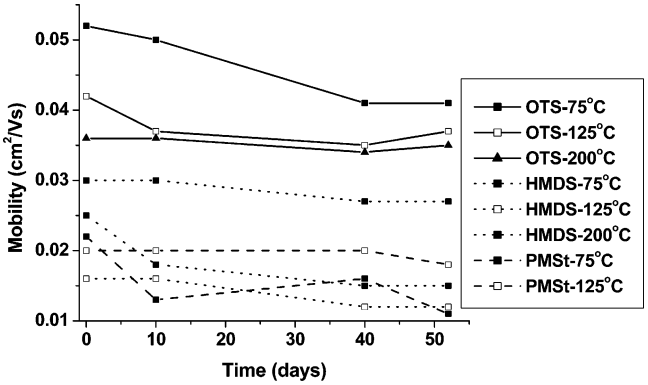

Figure 6. OTFT electron mobilities of **8** for $V_d = 100$ V as a function of time for devices exposed to air. The organic semiconductor films were grown on Si/SiO_2 substrates with different surface treatment at various substrate temperatures.

stability clearly suggests that *n*-channel organic semiconductors with lower LUMO levels tend to have better air stability.

Figure 6 shows electron mobilities of compound **8** with different surface treatment and substrate temperature used during deposition at $V_d = 100$ V as a function of time after being exposed to air. It appears that the surface treatment makes no obvious difference in air stability for TFT mobility. However, with the same surface treatment, the air stability is enhanced with increasing substrate temperatures, possibly due to the reduced number of grain boundaries and less trapping density for films with larger grains formed at elevated temperatures. In some cases, a slight increase in mobility was observed at a certain time. This may be related to the fluctuation in ambient humidity level over time, and it has been reported that high humidity levels reduce OTFT mobility.[23]

We further compare the TFT performance between unsubstituted compound **1** and substituted compound **8** with penta-F substituents in both nitrogen and air over time. The transfer traces ($I_d - V_g$) of TFTs from **1** using OTS−SiO_2 substrates grown at $T_s = 125$ °C and **8** grown at $T_s = 75$ °C at $V_d = 100$ V are shown in Figure 7. The tests were carried out in a nitrogen glove box after the devices were prepared, then under ambient conditions after the devices were exposed to air for a certain amount of time, followed by storage in the nitrogen glove box again. It can be seen that **1** showed good *n*-channel TFT performance when tested in a nitrogen glove box, but the performance deteriorated rapidly after the device was exposed to air for 1 h. Finally, almost no TFT activity was observed after the device was exposed in air for 3 days. However, if the same TFT was placed back in a dry nitrogen environment for some time to remove the oxygen adsorbed from air, its TFT performance was restored only partially even after 15 days, possibly due to the difficulty in complete removal of the adsorbed oxygen from the device. In contrast, TFT performance of compound **8** changed only slightly after the device was exposed to air for 1 h and changed little over time after being exposed to air for as long as 52 days (further monitoring is in progress). Also, its TFT performance can be completely restored after

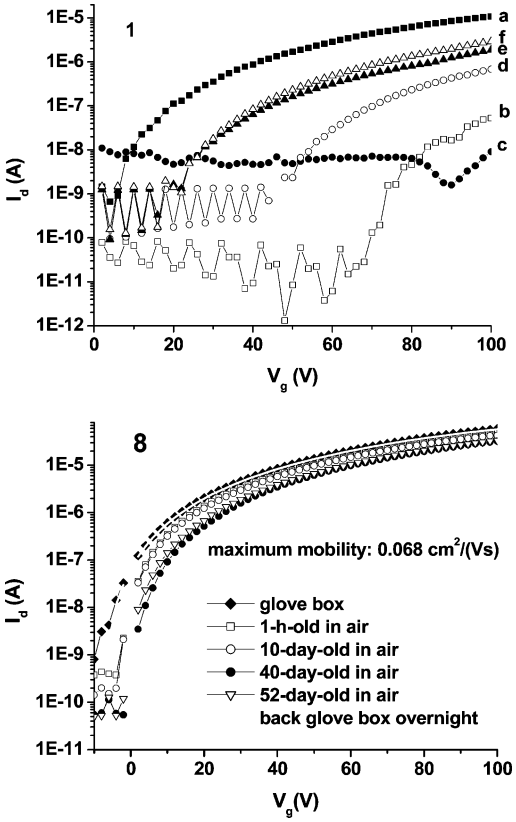

Figure 7. Transfer traces ($I_d - V_g$) of OTFTs on OTS treated SiO_2/Si substrates with **1** grown at $T_s = 125$ °C and **8** at $T_s = 75$ °C at $V_d = 100$ V. The data for **1** TFT were collected in a nitrogen glove box immediately after the device was prepared (a), under ambient conditions after the device was stored in an ambient atmosphere for 1 h (b) or 3 days (c), and again in the glove box after the device was put back inside a dry N_2 glove box for 1 h (d), 3 days (e), and 15 days (f). The data for **8** were collected in a dry nitrogen glove box under ambient conditions after the device was exposed to air for 1 h, 10 days, 40 days, and 52 days, and after being placed back inside a dry N_2 glove box overnight.

the device was put back into the nitrogen glove box overnight. Similar results were also observed for **8** TFTs grown on OTS−SiO_2 substrates at substrate temperatures of 125 and 200 °C.

All of the previous observations indicate that oxygen in air is mainly responsible for the *n*-channel device instability in air. This agrees with the accepted explanation of the device degradation in air for *n*-channel materials. Fluorination, however, can improve OTFT performance through lowering the LUMO energy levels, thus making them less susceptible to oxidation in the presence of oxygen in ambient environment. The compound with the most F substitution has the lowest LUMO level, the highest electron mobility, and the best TFT air stability.

Conclusion

In summary, a series of *n*-channel organic semiconductors based on perylene diimides were synthesized by introducing electron-withdrawing groups of CF_3, F, and Cl and by changing their position and number. OTFT performance from these perylene diimide derivatives depends heavily on both the type and the number of the substituents. Among the mono-substituted derivatives, **9** with the CF_3 groups gave the best TFT air stability, while **10** with the Cl group was

(23) Li, D. W.; Borkent, E. J.; Nortrup, R.; Moon, H.; Katz, H.; Bao, Z. N. *Appl. Phys. Lett.* **2005**, *86*, 042105.

the worst. Both OTFT mobility and air stability were improved in general by increasing the number of substituted fluorine groups. Compound **8** with penta-F substituents had a much higher mobility and better TFT air stability than compounds with a mono-F group. We think that the better air stability in the compounds with more fluorine substituents is due to their lower LUMO energy levels. Mobility as high as 0.068 cm^2/V s, on/off current ratio over 10^5, and threshold voltage as low as 0.4 V were obtained for **8** with penta-F substituents grown on the OTS−SiO_2 substrate at a low substrate temperature for deposition of 75 °C. The mobility of compound **8** does not change much after the device has been exposed to air for at least 72 days, showing that it is a promising air stable *n*-channel organic semiconductor for OTFTs and organic complementary circuits.

Acknowledgment. This work was supported by the National Natural Science Foundation of China (50225312, 50433020, and 50520150165) and by the China Scholarship Council. The work was also partly supported by Stanford School of Engineering and Stanford Center of Integrated Systems. The authors also thank Dr. Jason Locklin for helpful discussions.

Supporting Information Available: Syntheses and material characterization, XRD patterns, and AFM images. This material is available free of charge via the Internet at http://pubs.acs.org.

CM062352W